

Supplementary Information

Quaternary climate change drives allo-peripatric speciation and refugial divergence in the *Dysosma versipellis-pleiantha* complex from different forest types in China

Yi-Han Wang¹, Hans Peter Comes², Ya-Nan Cao¹, Rui Guo¹, Yun-Rui Mao¹ & Ying-Xiong Qiu^{1*}

¹Key Laboratory of Conservation Biology for Endangered Wildlife of the Ministry of Education, and Laboratory of Systematic & Evolutionary Botany and Biodiversity, College of Life Sciences, Zhejiang University, Hangzhou 310058, China, ²Department of Ecology and Evolution, Salzburg University, A-5020 Salzburg, Austria

*Corresponding author. Ying-Xiong Qiu. E-mail: qyxhero@zju.edu.cn

Supplementary Methods

Reconstruction of phylogenetic cpDNA haplotype trees

The best-fit substitution model employed was GTR+G as determined by Akaike Information Criteria (AIC) implemented in JMODELTEST (v1.1; Posada, 2008). The ML analysis was conducted using RAXML (v7.2.8; Stamatakis *et al.*, 2008) at the CIPRES SCIENCE GATEWAY (v3.1; Miller *et al.*, 2010). Nodal support was assessed using 1000 ‘fast bootstrap’ replicates. The BI analyses were performed using MRBAYES (v3.1.2; Ronquist & Huelsenbeck, 2003). Two independent Markov chain Monte Carlo (MCMC) runs were carried out with four differentially heated chains for 50 million generations, starting from a random tree. Model parameters were estimated during the analysis. Chains were sampled every 5000 generations. Convergence of the analyses was validated by (1) the standard deviation of the partition frequency [SD(s)] across runs (< 0.01); and (ii) monitoring the likelihood values over time using TRACER (v1.6.1; Drummond & Rambaut, 2007). The first 25% of generations were discarded as burn-in. A 50% majority-rule consensus tree was constructed from the remaining trees to estimate posterior probabilities (PPs).

MDA analysis

For each model analysis, goodness-of-fit based on the sum of squared deviations (*SSD*) and Harpending’s (1994) raggedness index (H_{Rag}) was tested using parametric bootstrapping (Schneider & Excoffier, 1999) with 1000 pseudoreplicates. Their *P* values represented the probability of obtaining a simulated *SSD* value (or H_{Rag}) greater than or equal to the observed one. For two expanding lineages identified, the

MDA-derived expansion parameter (τ), and its 95% confidence interval (CI), were converted to absolute estimates of time since expansion using $\tau = 2ut$ (Rogers & Harpending, 1992; Rogers, 1995), where u is the neutral mutation rate for the entire sequence per generation (Won & Hey, 2005). The value for u was calculated as $u = \mu kg$, where μ is the substitution rate in substitutions per site per year (here, 1.3×10^{-9} s/s/y), k is the average sequence length of the cpDNA region in this study (here, 2669 bp; see the Results section), and g is the generation time in years [i.e. age of first reproduction; approximately three years, observed for *D. versipellis* in cultivation at the Botanic Garden of Zhejiang University (Qiu *et al.*, 2005)].

Detection of null alleles, HWE and LD

For the EST-SSR dataset, all 15 genotyped loci were checked for frequencies of null alleles in FREENA (Chapuis & Estoup, 2007) following the Expectation Maximization (EM) method described by Dempster *et al.* (1977). Deviations from Hardy-Weinberg equilibrium (HWE) were tested using GENEPOP (v4.0.7; Rousset, 2008). Linkage disequilibrium (LD) among loci was tested using FSTAT (v2.9.3; Goudet, 2001). Statistical significance ($\alpha = 0.05$) for inferring LD or departures from HWE was evaluated based on 1000 permutations, and corrected for multiple tests using the sequential Bonferroni method (Rice, 1989).

STRUCTURE analysis

This program was run 10 times for a number of clusters (K), ranging from 2 to 40, using a burn-in length of 100,000 and run length of 500,000 iterations. We plotted the

probability of the data $[\ln P(D)]$ and the ad hoc statistic ΔK (Evanno *et al.*, 2005) to determine the most likely K .

MIGRATE-N analysis

These analyses were run for three replicates assuming a stepwise mutation model (Estoup *et al.*, 2002) with constant mutation rates for all loci. The initial run used an estimate of F_{ST} as a starting parameter to calculate M and each subsequent run used the ML estimates from the previous run as new starting parameters. For each run, we used uniform priors and Metropolis-coupled MCMC with 10 short chains and five long chains with 10,000 and 100,000 sampled genealogies, respectively, and set a static heating scheme at four temperatures (1, 1.3, 3 and 10). Genealogies were recorded every 50 steps and the first 10,000 were discarded as burn-in.

ABC analysis

For each of the eight models, we generated a reference table with 1×10^6 simulated data sets based on a divergence history that describes the model. All parameters that define each model (i.e. effective population size, divergence times and mutation rate) were considered as random variables with uniform distributions. For each simulation, the parameter values are drawn from their prior distributions, defining a divergence history that is used to construct a specific input file for the DIYABC program. The summary statistics of genetic variation were as follows: the mean number of alleles, mean expected heterozygosity (H_E) and mean allele size variance for each group, the overall F_{ST} , the classification indices (analogous to genotype assignment likelihoods),

and the shared allelic distance between pairs of groups. For both analyses, the prior distribution of mutation rates (μ , per generation per locus) for the EST-SSRs was assumed to be broad [1×10^{-6} , 1×10^{-3}] because they likely evolve more slowly than anonymous SSRs (Ellis & Burke, 2007). Likewise, a broad gamma distribution [1×10^{-1} , 9×10^{-1}] was specified for the parameter of the geometric distribution (P) to generate multiple stepwise mutations. However, for the effective population size and divergence time parameters, we employed different priors in the two steps (see details in Table 4). The average generation time was assumed to be three years (see MDA above). To compare the posterior probability of the four scenarios in each step, the 40,000 (1% proportion) simulated datasets closest to the observed dataset were selected for a polychotomous logistic regression approach (Cornuet *et al.*, 2008, 2010) and 4,000 for the direct estimate approach. For the best supported scenario, we estimated the posterior distributions of all parameters using a local linear regression on the 100,000 simulated datasets closest to the observed dataset, after the application of a logit transformation to parameter values (Beaumont *et al.*, 2002; Cornuet *et al.*, 2008). Finally, to evaluate whether the most fitting model successfully reproduced the observed data, we performed model-checking computations by simulating 100,000 pseudo-observed data sets from the posterior distribution of all parameters. Following Cornuet *et al.* (2010), we also conducted a principal component analysis (PCA) to test statistical vectors and visualize the consistency between simulated and observed data sets, using summary statistics that had not been used for model selection in the previous ABC treatments.

Supplementary Figures

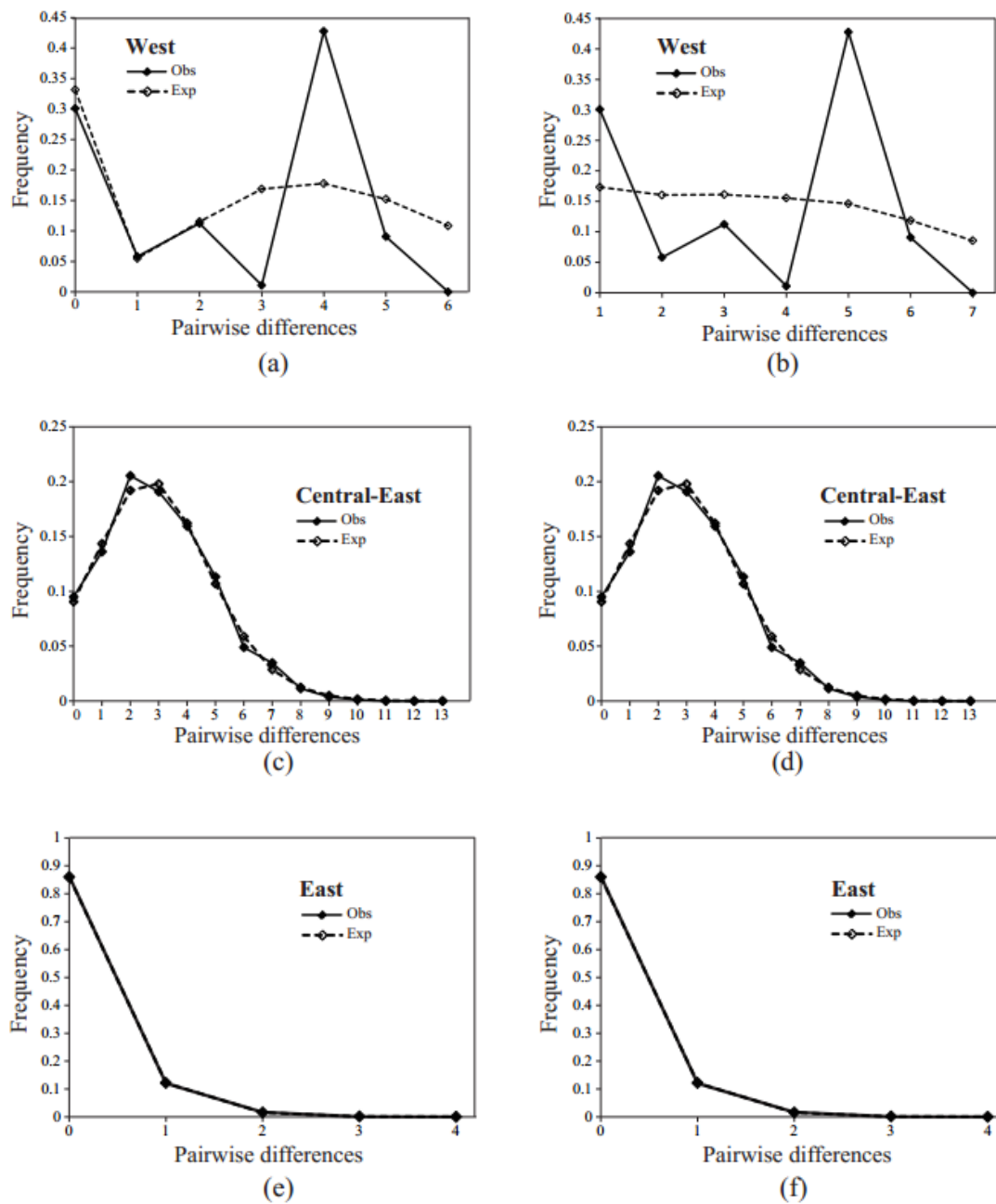


Figure S1. Mismatch distribution analyses (MDAs) of the three cpDNA lineages of the *Dysosma versipellis-pleiantha* complex (west, central-east: *D. versipellis s. lat.*; east: *D. pleiantha*) for the pure demographic expansion model (a, c, and e) and the spatial expansion model (b, d, and f).

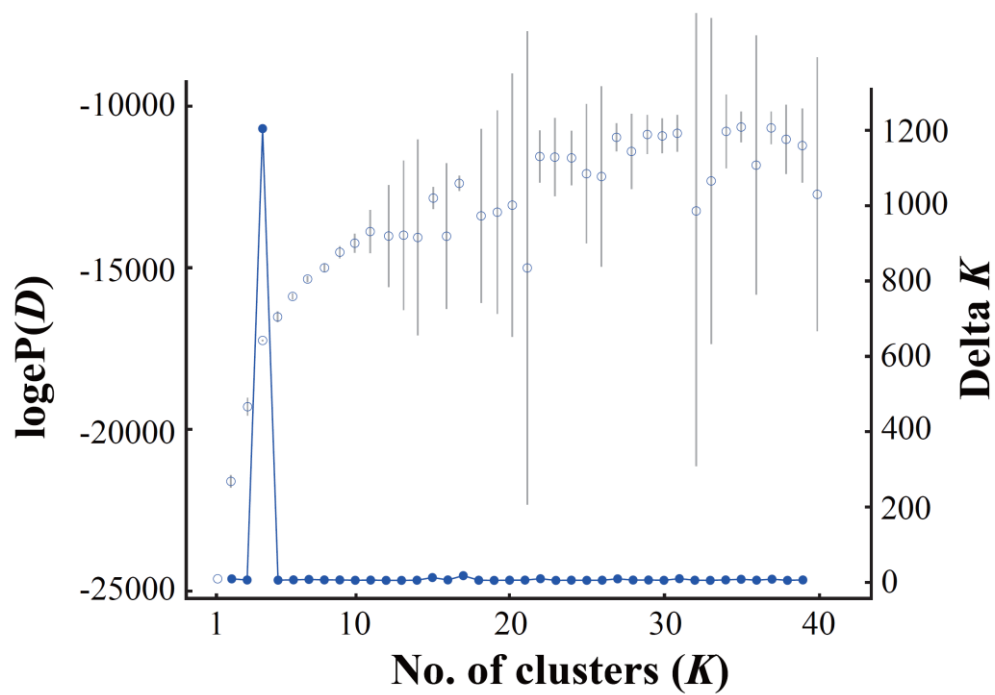


Figure S2. Changes of the mean posterior probability [$\ln P(D)$] (\pm SD) values of each K calculated according to Pritchard *et al.* (2000) (dot plot); and the corresponding ΔK statistics calculated according to Evanno *et al.* (2005) (line diagram) in the STRUCTURE analysis based on 15 EST-SSR loci.

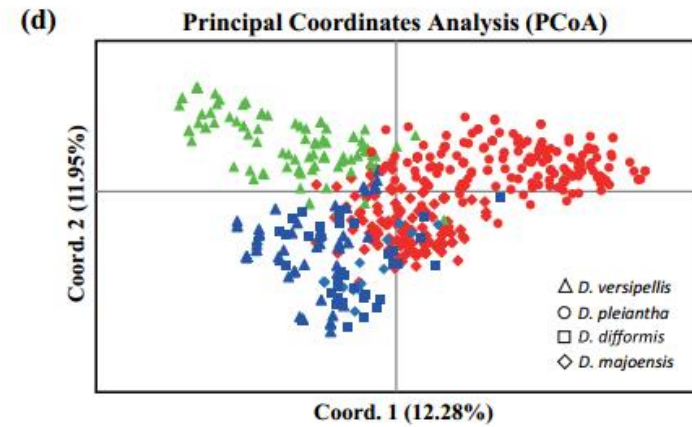
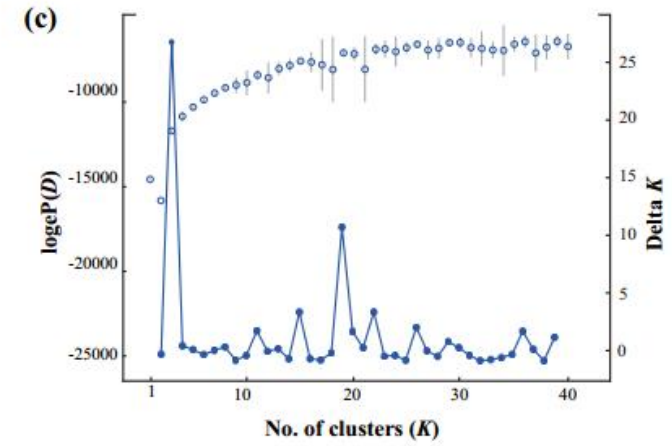
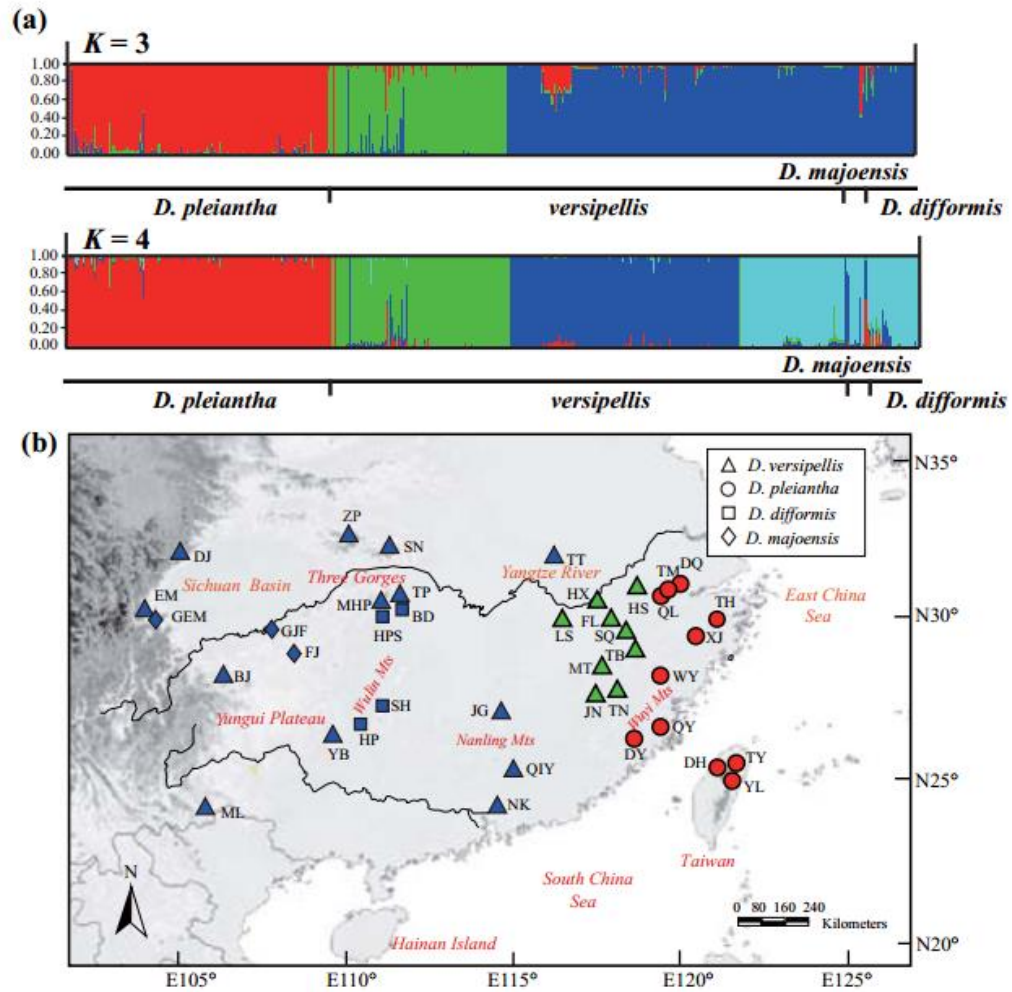


Figure S3. (a) Results of the STRUCTURE assignment test at $K = 3$ and $K = 4$ for 40 populations of the *Dysosma versipellis-pleiantha* complex based on genetic variation at nine neutral EST-SSR loci. (b) Geographic origin of each *Dysosma* population and their color-coded grouping according to the STRUCTURE analysis at $K = 3$ created in ILLUSTRATOR v15.0 (<http://www.adobe.com/products/illustrator.html>). The symbol next to each sampling locality identifies the respective *Dysosma* species, while the filled color represents the cluster assigned to that population (population codes are identified in Table S2). The base map was drawn using ARCGIS v.9.3 (ESRI, Redlands, CA, USA). (c) Changes of the mean posterior probability [$\ln P(D)$] (\pm SD) values of each K calculated according to Pritchard *et al.* (2000) (dot plot); and the corresponding ΔK statistics calculated according to Evanno *et al.* (2005) (line diagram) based on the nine neutral EST-SSR loci. (d) Principal coordinates analysis (PCoA) of the 577 individuals from the four species of the species complex based on EST-SSR variations (nine neutral loci).

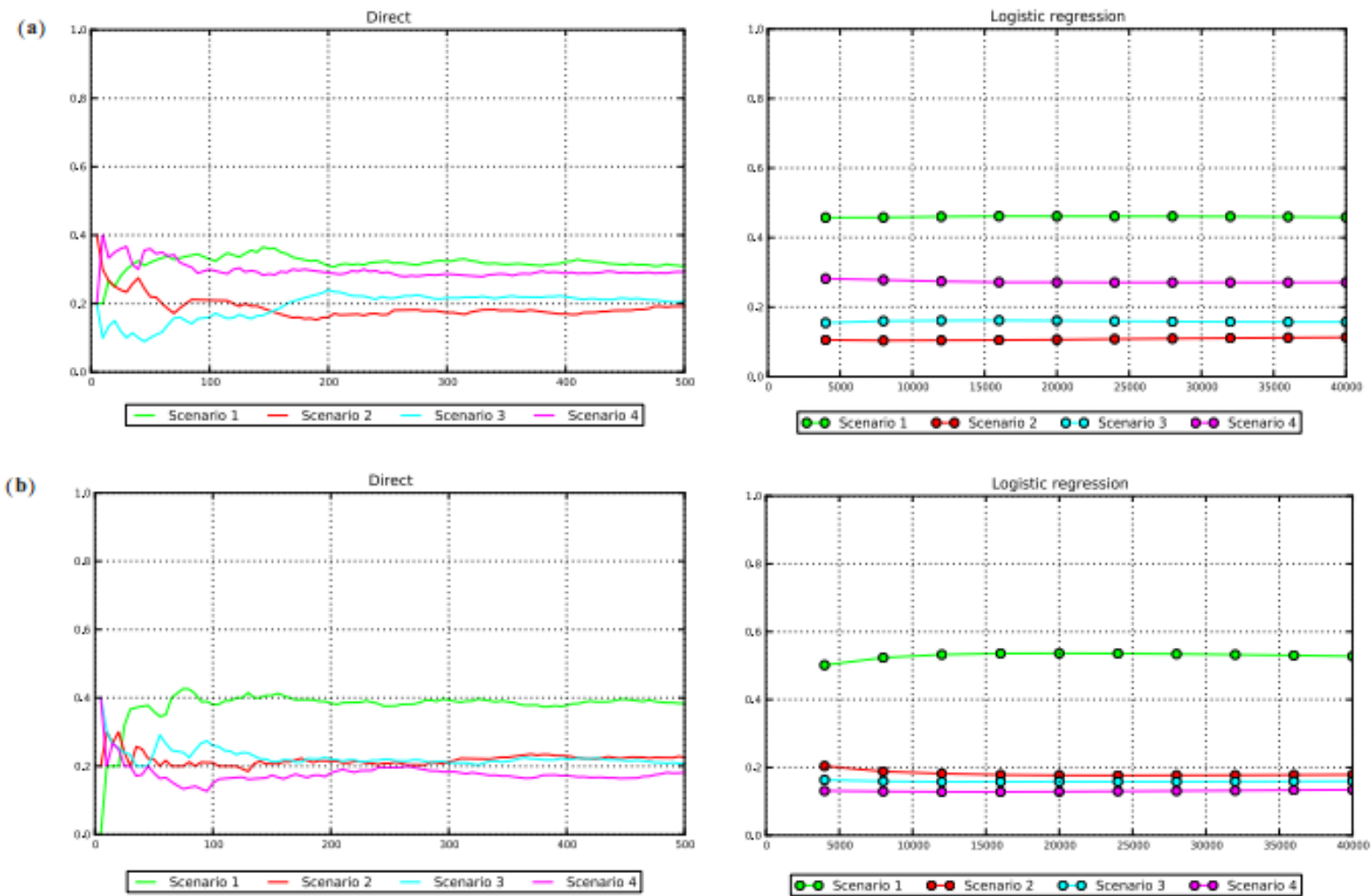


Figure S4. ABC model selection results using direct estimate and multinomial logistic regression approaches.

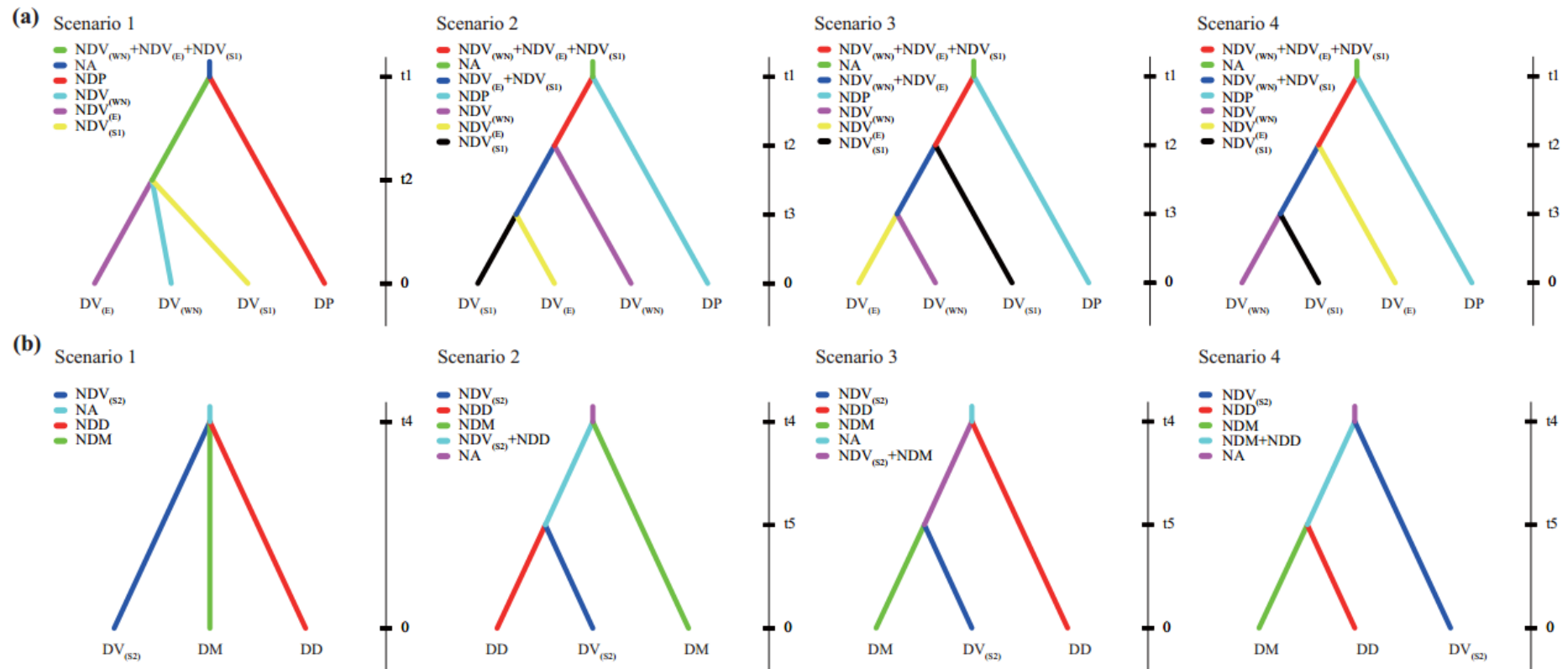


Figure S5. ABC modeling of scenarios for the diversification history of (a) the three regional EST-SSR (STRUCTURE) clusters of *Dysosma versipellis s. lat.* (west-north, east, south); and (b) the three taxonomic units of its ‘southern cluster’, i.e. *D. versipellis* (south), *D. difformis*

and *D. majoensis*. Divergence times (t_1-t_5 ; not to scale) are indicated and effective population sizes are marked in different colours. For parameter codes and scenario descriptions, see Table 4 and Supplementary Table S5, respectively.

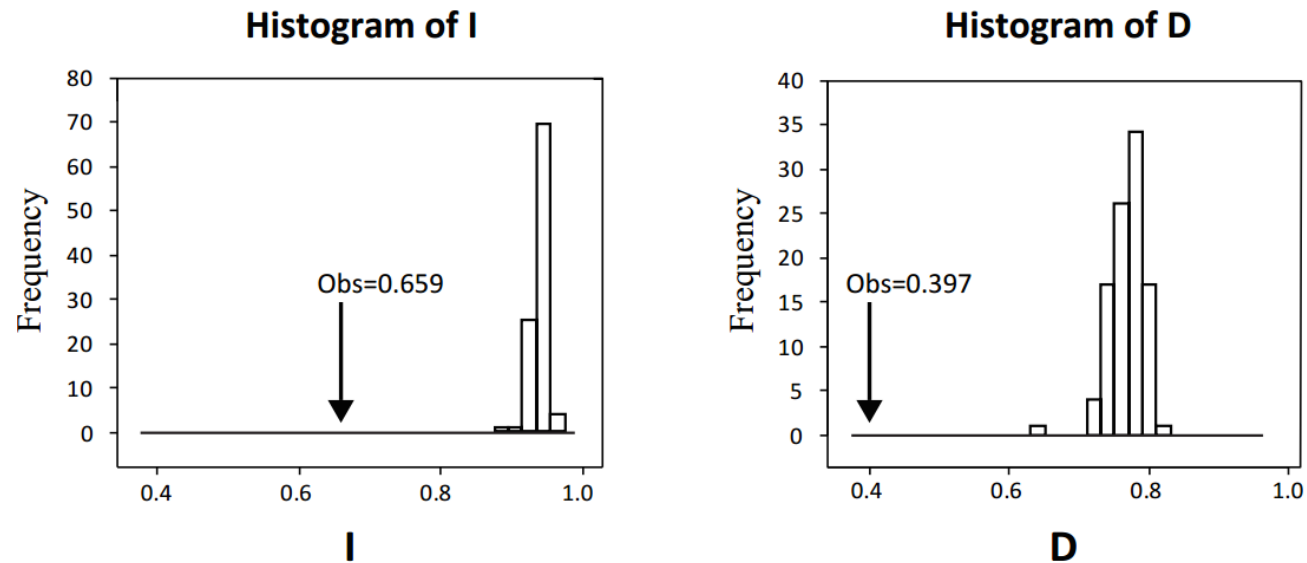


Figure S6. The results of identity tests between *Dysosma versipellis s. lat.* and *D. pleiantha* inhabiting, respectively, warm temperate deciduous (WTD) and warm temperate evergreen (WTE) forest in subtropical China. Bars indicate the null distributions of the standardized Hellinger distance (I) and Schoener's D , both generated from 100 randomizations. The x-axis indicates values of I and D , and the y-axis indicates the number of randomizations. The arrows indicate values of the actual MAXENT runs.

Table S2. Geographic and genetic characteristics of *Dysosma* population samples used in this study. n , number of individuals; h , haplotype diversity; π , nucleotide diversity; N_A , number of alleles; A_R , allele richness; H_E , expected heterozygosity; F_{IS} , fixation index.

Species/ Population code	Locality	Latitude (N)	Longitude (E)	Altitude (m)	n (cpDNA/EST-SSR)	cpDNA			EST-SSR (All 15 loci/nine neutral loci)			
						h (\pm SD)	$\pi \times 10^{-3}$ (\pm SD)	haplotypes	N_A	A_R	H_E	F_{IS}
<i>Dysosma versipellis</i>												
EM	Mt. E'mei, Sichuan Province	29°35'	103°21'	1200	12/23	0.167	0.13	H6, H7	44/28	1.274/1.307	0.274/0.307	-0.014/-0.102
DJ	Dujiangyan, Sichuan Province	31°06'	103°38'	1290	11/21	0.491	0.29	H2–H5	38/25	1.403/1.393	0.396/0.386	-0.756/-0.714
JF	Mt. Jinfo, Chongqing City	29°10'	107°10'	1650	12/–	0.167	0.60	H35, H36	–	–	–	–
ML	Malipo, Yunnan Province	23°07'	104°45'	1805	11/11	0.182	0.07	H1, H46	24/13	1.102/1.105	0.101/0.103	-0.138/-0.373
NG	Mt. Nangong, Shanxi Province	32°15'	109°04'	1800	10/–	0.556	0.34	H19, H20	–	–	–	–
SN	Shennongjia, Hubei Province	31°28'	110°22'	2000–2700	10/33	0	0	H18	56/39	1.457/1.496	0.459/0.497	0.212/0.161
TP	Mt. Tianping, Hunan Province	29°08'	110°28'	1000	10/14	0.712	0.50	H8, H9, H26, H27	38/24	1.403/1.422	0.402/0.421	-0.077/-0.055
TT	Tiantangzhai, Anhui Province	31°14'	115°74'	900–1200	18/36	0.837	0.74	H28–H34	47/29	1.257/1.292	0.257/0.292	-0.029/-0.061
HS	Mt. Huang, Anhui Province	30°08'	118°18'	800–1000	10/16	0.757	0.93	H1, H11–H15	37/24	1.275/1.316	0.275/0.316	0.028/0.012

HX	Haixing, Jiangxi Province	29°55'	116°87'	800	12/11	0.318	0.20	H9, H14, H16	36/24	1.293/1.386	0.296/0.391	0.219/0.246
FL	Fuliang, Jiangxi Province	29°55'	117°66'	800	10/2	0.511	0.22	H8–H10	25/16	1.344/1.463	0.304/0.406	0.059/0.077
SQ	Mt. Sanqing, Jiangxi Province	28°54'	118°03'	800	18/26	0.386	0.28	H1, H23, H24	44/31	1.350/1.468	0.351/0.470	0.174/0.190
TB	Mt. Tongba, Jiangxi Province	28°05'	118°15'	700–900	8/8	0	0	H1	22/14	1.203/1.299	0.192/0.278	-0.783/-1.000
JG	Mt. Jinggang, Jiangxi Province	26°28'	114°13'	300–500	11/11	0	0	H37	26/17	1.212/1.226	0.208/0.222	-0.422/-0.354
QIY	Mt. Qiyun, Jiangxi Province	25°46'	113°57'	570	14/13	0.495	0.43	H38–H41	31/24	1.276/1.403	0.274/0.401	-0.200/-0.130
NK	Mt. Nankun, Guangdong Province	32°15'	109°04'	1800	17/19	0	0	H42	28/18	1.195/1.165	0.195/0.165	-0.093/-0.015
YB	Mt. Yuanbao, Guangxi Province	25°26'	109°09'	1400	14/17	0	0	H1	38/22	1.374/1.382	0.373/0.384	-0.063/0.166
JN	Jianning, Fujian Province	26°55'	116°41'	500–700	19/29	0.368	0.15	H43–H45	37/24	1.215/1.208	0.216/0.209	0.048/0.223
MHP	Mt. Huping, Hunan Province	30°01'	110°32'	900–1200	7/11	0	0	H1	32/20	1.221/1.199	0.225/0.203	0.381/0.401
LS	Mt. Lu, Jiangxi Province	29°32'	115°59'	1082	10/11	0.644	0.37	H1, H12, H17	38/25	1.295/1.319	0.299/0.322	0.249/0.216
TN	Taining, Fujian Province	26°54'	117°10'	700	15/16	0	0	H43	30/19	1.157/1.162	0.157/0.162	-0.091/0.013
MT	Mt. Matou,	27°48'	117°08'		-/3	–	–	–	28/19	1.291/1.374	0.300/0.389	0.074/0.095

	Jiangxi province											
ZP	Zhenping county, Shanxi province	31°59'	109°20'		-/17	-	-	-	19/12	1.080/1.076	0.078/0.075	-0.856/-0.749
BJ	Bijie, Guizhou Province	27°24'	105°54'	1697	3/2	0	0	H56	18/11	1.133/1.148	0.100/0.111	-1.000/-1.000
Species mean						0.300 (0.29)	0.239 (0.27)		33/21	1.264/1.300	0.261/0.296	-0.140/-0.125
Species total						0.902	1.42		127/80	6. 403/6.795	0.619/0.635	0.529/0.503
<i>Dysosma pleiantha</i>												
TM	Mt. Tianmu, Zhejiang Province	30°19'	119°26'	400	19/26	0.450	0.22	H48–H51	58/42	1.412/1.464	0.414/0.465	0.188/0.141
DQ	Deqing, Zhejiang Province	28°54'	118°03'	400–500	9/36	0	0	H48	43/26	1.319/1.337	0.320/0.337	0.172/0.086
TH	Mt. Tiantai, Zhejiang Province	29°14'	120°00'	500	5/17	0	0	H47	42/31	1.372/1.489	0.374/0.492	0.152/0.158
XJ	Xianju, Zhejiang Province	28°42'	120°36'	500	8/8	0	0	H48	18/12	1.101/1.168	0.094/0.157	-0.765/-0.765
WY	Wuyanling, Zhejiang Province	27°41'	119°40'	1065	10/14	0	0	H48	39/26	1.323/1.387	0.323/0.385	0.030/-0.147

DY	Mt. Daiyun, Fujian Province	25°38'	118°11'	300	21/24	0	0	H48	45/33	1.320/1.481	0.320/0.481	0.045/0.027
QY	Mt. Qingyun, Fujian Province	26°01'	118°55'	600	19/23	0	0	H48	30/20	1.292/1.410	0.287/0.403	-0.770/-0.811
TY	County Taoyuan, Taiwan	24°43'	121°26'	1995	6/5	0	0	H48	26/15	1.289/1.267	0.287/0.267	-0.070/0.000
YL	County Yilan, Taiwan	24°34'	121°24'	1594/1699	18/13	0	0	H48	33/22	1.343/1.435	0.343/0.434	0.005/-0.064
DH	Mt. Dahun, Taiwan, China	24°41'	121°17'	1520	9/8	0	0	H48	37/26	1.362/1.468	0.358/0.460	-0.165/-0.237
QL	Mt. qingliang, Anhui province	30°06'	118°54'	600	-/4	–	–	–	25/17	1.258/1.333	0.298/0.434	0.032/0.123
Species mean						0.045	0.02		36/25	1.308/1.385	0.311/0.392	-0.104/-0.135
						(0.14)	(0.07)					
Species total						0.154	0.07		85/60	3.347/4.116	0.473/0.541	0.296/0.180
<i>Dysosma difformis</i>												
HP	Huaping, Guangxi Province	25°38'	109°54'	700	8/8	0	0	H1	45/29	1.481/1.494	0.500/0.507	0.491/0.381
HPS	Mt. Huping, Hunan Province	30°01'	110°32'	925	4/3	0.500	0.20	H1, H55	22/14	1.200/1.229	0.200/0.241	0.000/0.231

BD	Mt. Tianping, Hunan Province	29°45'	110°03'	1513	8/8	0	0	H55	33/20	1.419/1.455	0.412/0.444	-0.254/-0.375
SH	Mt. Shunhuang, Hunan Province	26°26'	110°58'	993	15/16	0.657	0.36	H1, H52–H54	52/31	1.431/1.435	0.432/0.439	0.070/0.280
Species mean						0.289 (0.34)	0.14 (0.17)		38/24	1.383/1.403	0.386/0.408	0.077/0.129
Species total						0.696	0.40		74/45	4.879/4.974	0.610/0.627	0.377/0.410
<i>Dysosma majoensis</i>												
FJ	Mt. Fanjing, Guizhou Province	27°56'	108°36'	942	6/6	0	0	H55	30/21	1.322/1.379	0.336/0.393	0.404/0.387
GJF	Mt. Jinfo, Chongqing	29°00'	107°11'	1823	5/5	0	0	H55	28/16	1.202/1.146	0.203/0.147	0.082/0.094
GEM	Mt. E'mei, Sichuan Province	29°35'	103°22'	2200	3/3	0	0	H55	24/16	1.289/1.311	0.244/0.305	0.122/-0.091
Species mean						0	0		27/18	1.271/1.278	0.261/0.282	0.203/0.130
Species total						0	0		48/33	3.014/3.548	0.447/0.464	0.523/0.512
All total						0.929	3.58		138/85	5.064/5.589		

Table S3. BEAST-derived estimates of $T_{MRC A}$ and their 95% highest posterior densities (HPDs) under two coalescent models (constant population-size and population expansion models) for relevant nodes of the Bayesian inference (BI) phylogeny of *Dysosma* (plus outgroups) based on cpDNA sequence data (see Fig. 2).

Node code	Descriptions of the corresponding clade	Model	
		Constant size (HPD 95%)	Expansion growth (HPD 95%)
Node A	<i>Dysosma</i> clade	4.14 (2.74–5.44) Ma	3.44 (2.30–4.68) Ma
Node B	<i>D. delavayi</i> and <i>D. versipellis-pleiantha</i> complex clade	3.33 (2.15–4.26) Ma	2.66 (1.74–3.63) Ma
Node C	<i>D. versipellis-pleiantha</i> complex	2.16 (1.33–2.72) Ma	1.66 (1.42–3.07) Ma
Node D	Western and eastern lineages	1.61 (0.81–2.09) Ma	1.23 (0.74–1.73) Ma
Node E	Central-eastern lineage	1.36 (0.81–1.68) Ma	1.02 (0.70–1.36) Ma
Node F	Western lineage	0.91 (0.33–1.27) Ma	0.70 (0.39–1.07) Ma
Node G	Eastern lineage	0.59 (0.11–0.88) Ma	0.52 (0.25–0.83) Ma

Table S4. Selective outliers identified by different F_{ST} -based neutrality test methods as implemented in LOSITAN, BAYESCAN and ARLEQUIN. Selective outliers are denoted by a plus sign (+) when the P -value was < 0.05 . Following a Bonferroni correction, selective outliers exhibiting significance are indicated by an asterisk (*).

Outlier detection method	Locus					
	Positive outlier			Balancing outlier		
	EDV-46	EDV-52	EDV-119	EDV-60	EDV-67	EDV-82
LOSITAN	+	*	+	*	*	*
BAYESCAN	*	*		+		
ARLEQUIN	*	*	+	*	*	+

Table S5. Four scenarios each tested by DIYABC modeling for the diversification history of (a) the three regional EST-SSR (STRUCTURE) clusters of *D. versipellis s. lat.* (west-north, east, south); and (b) the three taxonomic units of its ‘southern cluster’, i.e. *D. versipellis* (south), *D. difformis*, and *D. majoensis*. See also Supplementary Fig. S5 for scenario illustrations. Note that *D. pleiantha* was generally assumed as sister, based on the cpDNA haplotype network analysis (see Results, Fig. 1c). In (a), DP, DV_(WN), DV_(E), and DV_(S1) represent, respectively, *D. pleiantha*, *D. versipellis* west-north cluster, *D. versipellis* east cluster and *D. versipellis* south cluster (including *D. difformis* and *D. majoensis*). In (b), DV_(S2), DD, and DM represent, respectively, *D. versipellis* south cluster, *D. difformis* and *D. majoensis*.

Scenario	Description of divergence scenarios
(a)	
Scenario 1	DP and a common ancestor of DV _(E) , DV _(S1) and DV _(WN) diverged at t ₁ , and then DV _(E) , DV _(S1) and DV _(WN) diverged at t ₂ simultaneously.
Scenario 2	DP and a common ancestor of DV _(E) , DV _(S1) and DV _(WN) diverged at t ₁ , and then DV _(WN) and a common ancestor of DV _(S1) and DV _(E) diverged at t ₂ , finally, DM and DD diverged at t ₃ .
Scenario 3	DP and a common ancestor of DV _(E) , DV _(S1) and DV _(WN) diverged at t ₁ , and then DV _(S1) and a common ancestor of DV _(E) and DV _(WN) diverged at t ₂ , finally, DV _(E) and DV _(WN) diverged at t ₃ .
Scenario 4	DP and a common ancestor of DV _(E) , DV _(S1) and DV _(WN) diverged at t ₁ , and then DV _(E) and a common ancestor of DV _(S1) and DV _(WN) diverged at t ₂ , finally, DV _(S1) and DV _(WN) diverged at t ₃ .
(b)	
Scenario 1	DV _(S2) , DM and DD diverged at t ₄ simultaneously.
Scenario 2	DM and a common ancestor of DD and DV _(S2) diverged at t ₄ , then DD and DV _(S2) diverged at t ₅ .
Scenario 3	DD and a common ancestor of DM and DV _(S2) diverged at t ₄ , then DM and DV _(S2) diverged at t ₅ .
Scenario 4	DV _(S2) and a common ancestor of DD and DM diverged at t ₄ , then DD and DM diverged at t ₅ .

Table S6. Primer information of the five newly-developed EST-SSR markers used in this study.

Locus	Forward primer sequences (5'–3')	Reverse primer sequences (5'–3')	Repeated motif	Size range (bp)
EDV-81	CTCTGACGAATCATCCTCCTCTA	ACATTATGCTAGTGATGGCGTTT	(TTC) ₅	154–172
EDV-82	TACTGAGGGAGTTCCATGAGATG	CAACTCAAACCTTCTTCTGGGTA	(GGT) ₅	159–186
EDV-102	AGACGCTATAGAGTTTTACCGCC	ATCTTGAATTGAACCAGTCCGTA	(TGG) ₅	146–167
EDV-118	AGAGAGCTGATGCTAAGGTGTTG	ATCTTACTCTGCTGCCTCTGATG	(CTT) ₅	71–86
EDV-119	ACACCTTACGATCGACCTCCTAC	TCAACAAGTCTCAAAACCCAAC	(GCA) ₅	95–125

Table S7. GenBank accession numbers of all newly generated cpDNA haplotypes (including outgroups) identified within the *Dysosma versipellis-pleiantha* complex.

Species	Haplotype	GenBank accession number		
		<i>trnL-trnF</i>	<i>trnF-ndhJ</i>	<i>trnS-trnfM</i>
<i>D. versipellis/D. difformis</i>	H1	KT290738	KT290670	KT290806
<i>D. versipellis</i>	H2	KT290739	KT290671	KT290807
<i>D. versipellis</i>	H3	KT290740	KT290672	KT290808
<i>D. versipellis</i>	H4	KT290741	KT290673	KT290809
<i>D. versipellis</i>	H5	KT290742	KT290674	KT290810
<i>D. versipellis</i>	H6	KT290743	KT290675	KT290811
<i>D. versipellis</i>	H7	KT290744	KT290676	KT290812
<i>D. versipellis</i>	H8	KT290745	KT290677	KT290813
<i>D. versipellis</i>	H9	KT290746	KT290678	KT290814
<i>D. versipellis</i>	H10	KT290747	KT290679	KT290815
<i>D. versipellis</i>	H11	KT290748	KT290680	KT290816
<i>D. versipellis</i>	H12	KT290749	KT290681	KT290817
<i>D. versipellis</i>	H13	KT290750	KT290682	KT290818
<i>D. versipellis</i>	H14	KT290751	KT290683	KT290819
<i>D. versipellis</i>	H15	KT290752	KT290684	KT290820
<i>D. versipellis</i>	H16	KT290753	KT290685	KT290821
<i>D. versipellis</i>	H17	KT290754	KT290686	KT290822
<i>D. versipellis</i>	H18	KT290755	KT290687	KT290823
<i>D. versipellis</i>	H19	KT290756	KT290688	KT290824
<i>D. versipellis</i>	H20	KT290757	KT290689	KT290825
<i>D. versipellis</i>	H21	KT290758	KT290690	KT290826
<i>D. versipellis</i>	H22	KT290759	KT290691	KT290827
<i>D. versipellis</i>	H23	KT290760	KT290692	KT290828
<i>D. versipellis</i>	H24	KT290761	KT290693	KT290829
<i>D. versipellis</i>	H25	KT290762	KT290694	KT290830
<i>D. versipellis</i>	H26	KT290763	KT290695	KT290831
<i>D. versipellis</i>	H27	KT290764	KT290696	KT290832

<i>D. versipellis</i>	H28	KT290765	KT290697	KT290833
<i>D. versipellis</i>	H29	KT290766	KT290698	KT290834
<i>D. versipellis</i>	H30	KT290767	KT290699	KT290835
<i>D. versipellis</i>	H31	KT290768	KT290700	KT290836
<i>D. versipellis</i>	H32	KT290769	KT290701	KT290837
<i>D. versipellis</i>	H33	KT290770	KT290702	KT290838
<i>D. versipellis</i>	H34	KT290771	KT290703	KT290839
<i>D. versipellis</i>	H35	KT290772	KT290704	KT290840
<i>D. versipellis</i>	H36	KT290773	KT290705	KT290841
<i>D. versipellis</i>	H37	KT290774	KT290706	KT290842
<i>D. versipellis</i>	H38	KT290775	KT290707	KT290843
<i>D. versipellis</i>	H39	KT290776	KT290708	KT290844
<i>D. versipellis</i>	H40	KT290777	KT290709	KT290845
<i>D. versipellis</i>	H41	KT290778	KT290710	KT290846
<i>D. versipellis</i>	H42	KT290779	KT290711	KT290847
<i>D. versipellis</i>	H43	KT290780	KT290712	KT290848
<i>D. versipellis</i>	H44	KT290781	KT290713	KT290849
<i>D. versipellis</i>	H45	KT290782	KT290714	KT290850
<i>D. versipellis</i>	H46	KT290783	KT290715	KT290851
<i>D. pleiantha</i>	H47	KT290784	KT290716	KT290852
<i>D. pleiantha</i>	H48	KT290785	KT290717	KT290853
<i>D. pleiantha</i>	H49	KT290786	KT290718	KT290854
<i>D. pleiantha</i>	H50	KT290787	KT290719	KT290855
<i>D. pleiantha</i>	H51	KT290788	KT290720	KT290856
<i>D. difformis</i>	H52	KT290789	KT290721	KT290857
<i>D. difformis</i>	H53	KT290790	KT290722	KT290858
<i>D. difformis</i>	H54	KT290791	KT290723	KT290859
<i>D. difformis/D. majoensis</i>	H55	KT290792	KT290724	KT290860
<i>D. versipellis</i>	H56	KT290793	KT290725	KT290861
<i>D. delavayi</i> voucher 60		KT290794	KT290726	KT290862
<i>D. delavayi</i> voucher 61		KT290795	KT290727	KT290863
<i>D. delavayi</i> voucher 62		KT290796	KT290728	KT290864

<i>D. delavayi</i> voucher 63	KT290797	KT290729	KT290865
<i>D. delavayi</i> voucher 64	KT290798	KT290730	KT290866
<i>D. delavayi</i> voucher 65	KT290799	KT290731	KT290867
<i>D. delavayi</i> voucher 66	KT290800	KT290732	KT290868
<i>D. aurantiocaulis</i> voucher YN1	KT290801	KT290733	KT290869
<i>D. aurantiocaulis</i> voucher YN2	KT290802	KT290734	KT290870
<i>D. tsayuensis</i>	KT290803	KT290735	KT290871
<i>Sinopodophyllum hexandrum</i>	KT290736	KT290668	KT290804
<i>Podophyllum peltatum</i>	KT290737	KT290669	KT290805

References

- Beaumont, M.A., Zhang, W. & Balding, D.J. Approximate Bayesian computation in population genetics. *Genetics* **162**, 2025-2035 (2002).
- Chapuis, M. & Estoup, A. Microsatellite null alleles and estimation of population differentiation. *Mol. Biol. Evol.* **24**, 621-631 (2007).
- Cornuet, J. et al. Inferring population history with DIY ABC: a user-friendly approach to approximate Bayesian computation. *Bioinformatics* **24**, 2713-2719 (2008).
- Cornuet, J., Ravigné, V. & Estoup, A. Inference on population history and model checking using DNA sequence and microsatellite data with the software DIYABC (v1. 0). *BMC Bioinform.* **11**, 1 (2010).
- Dempster, A.P., Laird, N.M. & Rubin, D.B. Maximum likelihood from incomplete data via the EM algorithm. *J. R. Stat. Soc. Series. B. Stat. Methodol.* **39**, 1-38 (1977).
- Drummond, A.J. & Rambaut, A. BEAST: Bayesian evolutionary analysis by sampling trees. *BMC Evol. Biol.* **7**, 214 (2007).
- Ellis, J.R. & Burke, J.M. EST-SSRs as a resource for population genetic analyses. *Heredity* **99**, 125-132 (2007).
- Estoup, A., Jarne, P. & Cornuet, J.M. Homoplasy and mutation model at microsatellite loci and their consequences for population genetics analysis. *Mol. Ecol.* **11**, 1591-1604 (2002).
- Evanno, G., Regnaut, S. & Goudet, J. Detecting the number of clusters of individuals using the software STRUCTURE: a simulation study. *Mol. Ecol.* **14**, 2611-2620 (2005).
- Goudet, J. FSTAT, version 2.9.3.2. A program to estimate and test gene diversities and fixation indices. <http://www2.unil.ch/popgen/siftwares/fstat.htm> (2001).
- Miller, M.A., Pfeiffer, W. & Schwartz, T. Creating the CIPRES Science Gateway for inference of large phylogenetic trees. Gateway Computing Environments Workshop (GCE), New Orleans, LA, USA (2010).
- Posada, D. jModelTest: phylogenetic model averaging. *Mol. Biol. Evol.* **25**, 1253-1256 (2008).
- Pritchard, J.K., Stephens, M. & Donnelly, P. Inference of population structure using multilocus genotype data. *Genetics* **155**, 945-959 (2000).

-
- Qiu, Y., Zhou, X., Fu, C. & Chan, Y.G. A preliminary study of genetic variation in the endangered, Chinese endemic species *Dysosma versipellis* (Berberidaceae). *Bot. Bull. Acad. Sinica.* **46**, 61–69 (2005).
- Rice, W.R. Analyzing tables of statistical tests. *Evolution* **43**, 223-225 (1989).
- Rogers, A.R. & Harpending, H. Population growth makes waves in the distribution of pairwise genetic differences. *Mol. Biol. Evol.* **9**, 552-569 (1992).
- Rogers, A.R. Genetic evidence for a Pleistocene population explosion. *Evolution* **49**, 608-615 (1995).
- Ronquist, F. & Huelsenbeck, J.P. MrBayes 3: Bayesian phylogenetic inference under mixed models. *Bioinformatics* **19**, 1572-1574 (2003).
- Rousset, F. Genepop'007: a complete re-implementation of the genepop software for Windows and Linux. *Mol. Ecol. Res.* **8**, 103-106 (2008).
- Schneider, S. & Excoffier, L. Estimation of past demographic parameters from the distribution of pairwise differences when the mutation rates vary among sites: application to human mitochondrial DNA. *Genetics* **152**, 1079-1089 (1999).
- Stamatakis, A., Hoover, P. & Rougemont, J. A rapid bootstrap algorithm for the RAxML web servers. *Syst. Biol.* **57**, 758-771 (2008).
- Won, Y. & Hey, J. Divergence population genetics of chimpanzees. *Mol. Biol. Evol.* **22**, 297-307 (2005).